Droplet ejection mechanism from tungsten electrode in multi-phase AC arc by high-speed visualization

T. Hashizume, M. Tanaka and T. Watanabe

Department of Chemical Engineering, Kyushu University, Fukuoka, Japan

Abstract: Droplet ejection in a multi-phase AC arc was observed by high-speed camera and appropriate band-pass filters system. According to the high-speed observation, larger droplets were ejected only at the cathodic period and the transition time from the cathodic to anodic AC period. The estimation of forces acting on the molten droplet revealed the electromagnetic force was the most important force for the droplet ejection.

Keywords: thermal plasmas, multi-phase AC arc, electrode erosion, droplet ejection

1. Introduction

Thermal plasmas as an energy source with high energy efficiency have been applied in various engineering fields. They have various advantages such as extremely high temperature, high enthalpy to enhance reaction kinetics, rapid quenching capability to produce chemical non-equilibrium materials, and oxidation or reduction atmosphere in accordance with required chemical reaction. Therefore, these advances increase demands in plasma chemistry and plasma processing [1-3].

The multi-phase AC arc is generated among multi-electrodes with large plasma volume by phase-shifted AC power supplies. The multi-phase AC arc can be generated without the intermittent discharge because the arc always exists among 12 electrodes. It has various advantages such as high energy efficiency, large plasma volume, low gas velocity compared with the conventional thermal plasmas [4-6]. The multi-phase AC arc is expected to be applied to massive powder processing such as nanomaterial fabrication processes and innovative in-flight glass melting technology. However, fundamental phenomena in multi-phase AC arc have rarely been reported because of its novelty. In particular, electrode erosion is one of the most important issues to be solved because it determines the electrode lifetime and the purity of the products. In multi-phase AC arc, the electrode erosion due to droplet ejection and evaporation was observed. According to the observation of the electrode phenomena, the electrode erosion by droplet ejection is significant.

The purpose of the present study is to understand the droplet ejection mechanism by high-speed observation of the electrodes. High-speed video camera with appropriate band-pass filters system was applied to visualize electrode phenomena in the multi-phase AC arc. The dynamic behavior of metal droplet ejection from the electrode surface was observed.

2. Experimental details

2.1 Experimental setup

Figure 1 shows a schematic image of the experimental setup. It consisted of 12 electrodes, arc chamber, and AC power supply at 60Hz. The electrodes were made of tungsten (98wt%) and thoria (2wt%) with diameter of 6.0 mm. The electrodes were divided into two layers, upper six and lower six electrodes. The electrodes were symmetrically arranged by the angle of 30 degree. To prevent the electrodes from oxidation, 99.99% argon was injected around the electrode as shield gas at 2-5 L/min of the flow rate. The applied voltage between each electrode and the neutral point of the coil of the transformer can be calculated by the following equation:

$$V_i = V_m \sin\left[\omega t - \frac{2\pi(i-1)}{12}\right] \quad (i = 1, 2, \ldots, 12) \qquad (1)$$

where V_i indicates the applied non-load voltage for each electrode number i and V_m indicates the amplitude of the non-load voltage (about 220 V, AC 60Hz). The arc current was changed from100 to 140 A for each electrode.

2.2 High-speed observation of electrode phenomena

Electrode phenomena in multi-phase AC arc were visualized by the high-speed camera system (FASTCAM

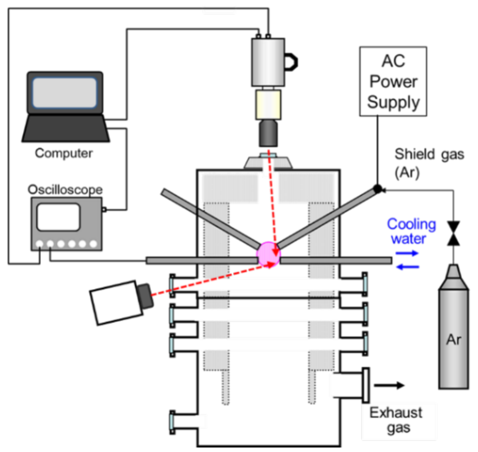

Fig. 1. Schematic image of multi-phase AC arc generator.

SA-5, Photron Ltd., Japan). Figure 2 shows a representative snapshot of multi-phase AC arc, which was taken from the top of the arc chamber. One of the electrodes was observed by high-speed camera installed on the top of the arc generator as shown in Fig. 2. Conventional observation of electrode during arc discharge was prevented by the strong emission of the arc. Therefore, the band-pass filters with 785 and 880 nm were combined with the high-speed camera system to separate the electrode thermal radiation from the emission of the arc. The clear visualization of electrode tip was achieved by the combination of high-speed camera and band-pass filters.

2.3 Temperature measurements of electrode surface

The electrode surface temperature was also measured by the same camera systems mentioned above. Based on two-color pyrometry, following equation was applied to calculate the surface temperature:

$$T = \frac{C_b(\lambda_1 - \lambda_2)}{\lambda_1 \lambda_2}\left[\ln R + 5\ln\left(\frac{\lambda_1}{\lambda_2}\right)\right]^{-1} \quad (2)$$

Temperature T was estimated from the ratio of thermal radiation intensities at different wavelengths λ_1 and λ_2.

3. Result and discussion

3.1 Droplet ejection during an AC cycle

High-speed camera observation revealed that the diameters of droplets ejected from the electrodes were distributed in the range from tens to several hundred micrometers.

Figure 3 shows time transient of the number of the ejected droplets during AC cycles. At the first half period, the electrode is in the anodic period whereas the second half corresponds to the cathodic period. Red plots with solid line indicate the total number of ejected droplets. Three peaks can be found at the anodic period, the cathodic period, and the transition time from the cathodic to anodic period. On the other hand, the blue plots with broken line in Fig. 3 indicate the number of the droplets larger than 250 μm in diameter. Only two peaks are found at the cathodic period and the transition time from the cathodic to the anodic period. This result suggests that the electrode erosion by droplet ejection mainly occurred at the cathodic period and the transition time from the cathodic to anodic period.

According to the observation of electrode tip during an AC cycle by the high-speed camera, the electrode tip in molten state became hemispherical shape forming a droplet pending on the electrode. Such pending droplet then detached from the electrode surface at the cathodic period. On the other hand, at the anodic period, the pending droplet became small returning to the electrode without detachment from the electrode tip. This different behavior of the molten part in the electrode tip led to large droplet ejection only at the cathodic period. The reason for this different behavior will be discussed in following section.

3.2 Force balance on the molten electrode

The electrode tip in molten state became hemispherical shape forming a pending droplet at the anodic and cathodic period. However the large droplet detached from molten electrode tip only at the cathodic period. The mechanism of the ejection of larger droplets is investigated by the evaluation of forces on the droplets pending on the electrode. Evaluations of the major forces acting on the molten tip are given in the following.

The force due to the surface tension, P_{st}, which pulls the electrode tip in molten state back is considered as in Eq. (3).

$$P_{st} = \frac{\sigma}{r} \quad (3)$$

where σ is the surface tension and r is the radius of the electrode tip in molten state.

The electromagnetic force, P_{em}, is caused by interaction of current flowing inside electrode tip with the self-induced magnetic field in the direction toward the center of the electrode. With the assumption that the axial

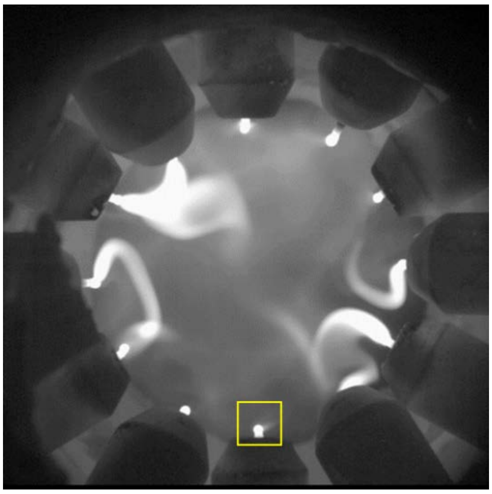

Fig. 2. Representative snapshot of multi-phase AC arc.

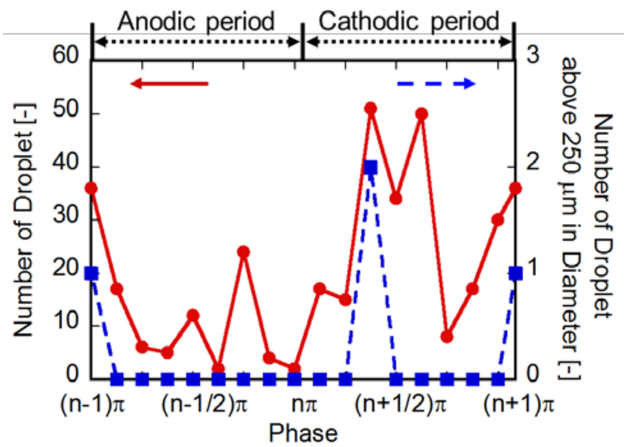

Fig. 3. Time transient of the number of the ejected droplets during AC periods at 60 Hz.

current density is distributed uniformly over any horizontal cross section of the droplet, the electromagnetic force is given by:

$$P_{em} = \frac{\mu_0}{8\pi} \frac{I^2}{r^2} \tag{4}$$

where μ_0 is magnetic permeability and I is the total arc current.

The pressure due to ion attack on the electrode surface should be considered at the cathodic period because the ion with positive charge is accelerated towards the electrode only at the cathodic period. The number of ions impacting the cathode per unit area and per unit time is:

$$n = \frac{\eta j}{e} \tag{5}$$

where j is the current density and e is the electron charge. η is the current fraction of the total current. The pressure is equal to the momentum change of these impacting ions:

$$P_{ion} = \eta j \sqrt{\frac{2 m_i V}{e}} \tag{6}$$

where m_{i} is the ion mass and V is the sheath voltage at the cathode. V is assumed to be 10 V. In the present evaluation, the ion current fraction was assumed to be 30 %, which is reasonable value reported in the previous studies about the electrode phenomena in DC arc torches with thoriated-tungsten cathode [7].

Figure 4 shows the evaluated forces on the molten electrode tip. Surface tension and ion pressure are the forces which pull the pending droplet back to the electrode side, resulting in suppress of droplet ejection. On the other hand, the electromagnetic force is the force squeezes and detaches the pending droplet from the electrode, resulting in the droplet ejection.

As shown in Eqs. (3) and (4), the surface tension and the electromagnetic force are proportional to r^{-1} and r^{-2}, respectively, where r is the radius of the droplet as indicated in the previous paragraph. Therefore, smaller radius of a pending droplet leads to stronger electromagnetic force than surface tension. Forces on the electrode tip are varied by the temperature fluctuation, the variation of the molten electrode shape and volume, current variation, and so on. Therefore, the dynamic behavior of the molten tip was observed by high-speed camera, and the forces on electrode tip at the cathodic and anodic period were evaluated.

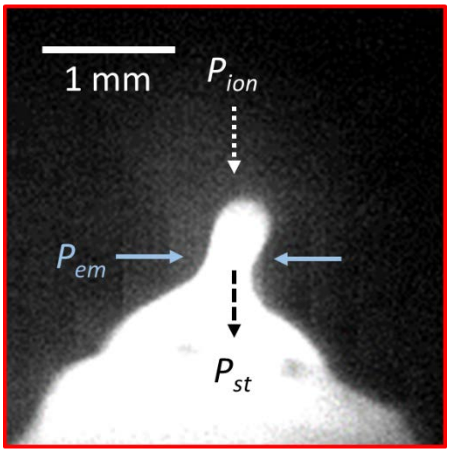

Fig. 4. Evaluated forces on molten electrode tip.

Figure 5 (a) shows the representative snapshots of the large droplet ejection during the cathodic period, and Fig. 5 (b) shows current and voltage waveforms synchronized with the high-speed observation. In addition, the time variation of the evaluated forces acting on the electrode tip during the cathodic period is shown in Fig. 5 (c). The waveforms and the evaluated forces including the high-speed snapshots were synchronized as indicated in Fig. 5 (a)-(c) from the synchronized waveform measurements with the high-speed observations. The surface tension and ion pressure are stronger than the electromagnetic force at most of the cathodic period. However, higher current led to stronger electromagnetic force, hence the molten electrode tip became hemispherical shape forming a pending droplet as shown in Fig. 5 (a)-(c). After the molten tip formed the pending droplet at 12.4 ms, the pending droplet diameter became smaller and the electromagnetic force became more important. The pending droplet finally detached from molten electrode tip at the time when the electromagnetic force became the dominant force at 13.4 ms.

The representative snapshots of the electrode tip during the anodic period and the synchronized waveforms of current and voltage are shown in Fig. 6 (a) and (b), respectively. Figure 6 (c) shows the time variation of the evaluated forces acting on the electrode tip during the anodic period, which is also synchronized with the waveforms. The heat transfer from the arc to the electrode at the anodic period is larger than that at the cathodic period. Therefore, the volume of the molten part in the electrode at the anodic period is larger than that at the cathodic period, and the surface tension is dominant force during the anodic period. As well as the cathodic period, the electrode tip became hemispherical shape forming a droplet pending on the electrode. However the pending droplet became small returning to the electrode without detachment from the electrode tip because the surface tension was dominant force.

The discussion in the previous paragraphs suggests that the droplet diameter on the electrode surface has important role to determine whether the pending droplet finally detaches from the electrode surface or not. The molten electrode tip becomes hemispherical shape forming the pending droplet at the cathodic and anodic period. However, only at the cathodic period, the electromagnetic force becomes dominant force and the pending droplet detaches due to smaller volume of the molten part in the electrode. In the case of stronger surface tension or ion pressure than the electromagnetic force, the pending droplet becomes small returning to the electrode without detachment from the electrode tip.

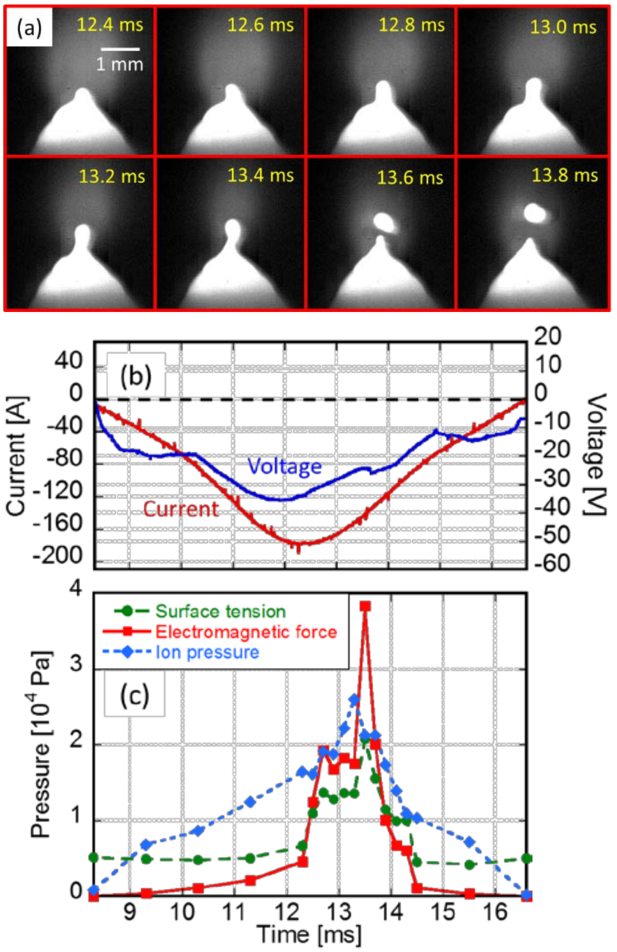

Fig. 5. Representative snapshots of molten electrode tip observed at cathodic period (a), synchronized current/voltage waveform (b), and time variation of the evaluated forces (c).

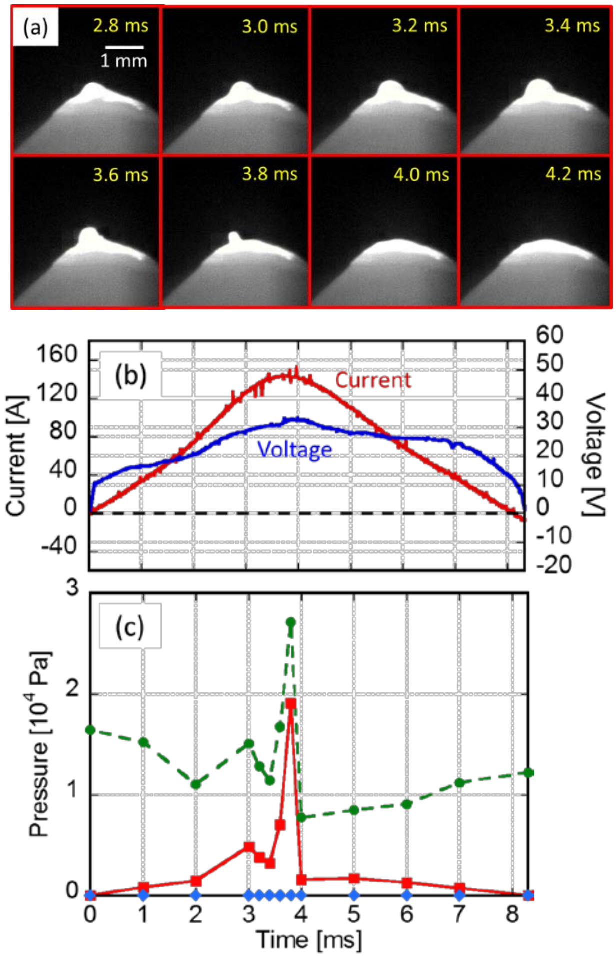

Fig. 6. Representative snapshots of molten electrode tip observed at anodic period (a), synchronized current/voltage waveform (b), and time variation of the evaluated forces (c).

4. Conclusions

The dynamic behavior of droplets ejection in the multi-phase AC arc was successfully visualized by the high-speed camera observation combined with the appropriate band-pass filters system. The effect of the polarity on the droplet ejection was investigated. The results indicated that the electrode erosion by the droplet ejection was mainly attributed to the droplets with diameter larger than 250 μm at the cathodic period and the transition time from the cathodic to anodic period. The mechanism of the ejection of larger droplets is investigated by the evaluation of forces on the droplet pending at the electrode. The correlation between the experimental results and the evaluated results of the forces suggests that the diameter of the droplet pending at the electrode tip is one of the most important parameter to determine the droplet ejection. Smaller diameter of the pending droplet leads to detachment of the droplet from the electrode surface due to relatively stronger electromagnetic force than surface tension. After the molten electrode tip becomes hemispherical shape forming a pending droplet, the pending droplet detaches from the electrode at the time when the electromagnetic force becomes the dominant force. Understanding the erosion mechanism in more details and decreasing the erosion rate enable to realize the practical use of the multi-phase AC arc in various applications.

5. References

[1] T. Watanabe, et al., *Plasma Chem. Plasma Process.*, 32, 123 (2012).

[2] M. Shigeta and T. Watanabe, *J. Phys. D: Appl. Phys.*, 40, 2407 (2007).

[3] M. Tanaka and T. Watanabe, *Jpn. J. Appl. Phys.*, 52, 076201 (2013).

[4] Y. C. Yao, et al., *Sci. Technol. Adv. Mat*, 9, 8 (2008).

[5] Y. Yao, et al., *Chem. Eng. J.*, 144, 317 (2008).

[6] Y. Yao, et al., *Chem. Eng. J.*, 139, 390 (2008).

[7] X. Zhou and J. Heberlein, *Plasma Sources Sci. Technol.*, 3, 564 (1994).